

## Proton Pickup from $^{86}\text{Sr}$ and the $^{85}\text{Rb}$ Level Structure\*

R. C. Ragaini

*University of California, Lawrence Livermore Laboratory, Livermore, California 94550*

J. D. Knight and W. T. Leland

*University of California, Los Alamos Scientific Laboratory, Los Alamos, New Mexico 87544*

(Received 7 May 1973)

The levels of  $^{85}\text{Rb}$  have been investigated by the  $^{86}\text{Sr}(t, \alpha)$  reaction with 15-MeV tritons.  $\alpha$ -particle spectra were measured by a  $\Delta E$ - $E$  counter telescope system with an over-all resolution of 50 keV. Angular distributions were measured from 12.5 to 90°, and comparison with distorted-wave Born-approximation calculations permitted angular momentum assignments for 11 of the 20 levels observed. The data are compared with previous information on the  $^{85}\text{Rb}$  level structure.

### I. INTRODUCTION

Although  $^{85}\text{Rb}$  is one of the more accessible nuclides from an experimental standpoint, until recently there have been relatively few data on its level structure.<sup>1</sup> Recent reports, however, have provided information from decay-scheme studies,<sup>2,3</sup> Coulomb-excitation experiments,<sup>4,5</sup> and ( $n'\gamma$ ) reaction studies.<sup>6</sup> In addition, a theoretical calculation<sup>7</sup> employing a Coriolis coupling model with the incorporation of a residual interaction of the pairing type has shown some success in accounting for the lower-lying level structure in the odd- $A$  rubidium isotopes.

We use the proton pickup reaction to study the proton-hole components of the  $^{85}\text{Rb}$  levels. Since the proton configuration of the  $^{86}\text{Sr}$  target nucleus can be approximated by the shell-model representation— $(1f_{7/2})^3(1f_{5/2})^6(2p_{3/2})^4$ , the  $^{85}\text{Rb}$  levels populated most strongly by proton pickup should have components of the type  $(1f_{5/2})^{-1}$ ,  $(2p_{3/2})^{-1}$ , and  $(1f_{7/2})^{-1}$ .

### II. EXPERIMENTAL PROCEDURE

We performed our experiments using 15-MeV incident tritons accelerated at the Los Alamos Scientific Laboratory tandem Van de Graaff facility. Triton-beam currents were typically 300 to 600 nA on target, with the beam spot approximately 1 mm<sup>2</sup>. The target consisted of ~75  $\mu\text{g}/\text{cm}^2$  of metallic strontium evaporated onto 50- $\mu\text{g}/\text{cm}^2$  carbon foil from  $\text{Sr}(\text{NO}_3)_2$ . The strontium had the following isotopic composition:  $^{86}\text{Sr}$ —97.6%,  $^{88}\text{Sr}$ —1.73%,  $^{87}\text{Sr}$ —0.68%,  $^{84}\text{Sr}$ —~0.05%. Careful examination of the reaction spectra showed no evidence of identifiable reactions on strontium isotopes other than  $^{86}\text{Sr}$ .

We measured all the particle spectra with a semiconductor  $\Delta E$ - $E$  counter telescope in conjunction with a particle identification system employing an on-line computer; construction and

operation of the over-all system are described in Refs. 8 and 9. Our  $\alpha$ -particle spectrum measurements were performed together with measurements of hydrogen isotope spectra, and we chose a  $\Delta E$  detector thickness of 400  $\mu$  to enhance the higher-energy parts of the latter spectra. Therefore, the  $\alpha$  particles were all stopped in the  $\Delta E$  detector and their spectra originated from this detector only. The  $\Delta E$ -originating spectra also contained events from lower-energy protons, deuterons, and tritons, as well as from  $^3\text{He}$  and any heavier ions, but all lay well below the energy range of interest, which contained only  $\alpha$  particles. Over-all system resolution for the  $\alpha$  particles was 50-keV full width at half maximum.

We determined excitation energies of the  $^{85}\text{Rb}$  levels by using an energy scale based on the following  $Q$  values<sup>10</sup>:

$$^{16}\text{O}(t, \alpha)^{15}\text{N}, \quad Q_0 = 7.6869 \pm 0.0006 \text{ MeV},$$

$$^{86}\text{Sr}(t, \alpha)^{85}\text{Rb}, \quad Q_0 = 10.1756 \pm 0.0028 \text{ MeV}.$$

We derived the target thicknesses used in the calculation of the absolute ( $t, \alpha$ ) cross sections from the analysis of the elastic scattering measurements.

### III. EXPERIMENTAL RESULTS

#### A. Triton Elastic Scattering

We measured triton elastic scattering angular distributions at 2.5° intervals from 10 to 100° and analyzed them using an optical-model potential of the Woods-Saxon type

$$U(r) = V_c - V[e^x + 1]^{-1} - i[W][e^{x'} + 1]^{-1} \quad (1)$$

where

$$x = (r - r_0 A^{1/3})/a,$$

$$x' = (r - r'_0 A^{1/3})/a',$$

TABLE I. Optical potentials in the distorted-wave analysis. The parameter  $r_0^c = 1.25$  and 1.30 fm for the tritons and  $\alpha$  particles, respectively.

| Type    | $V$<br>(MeV) | $r_0$<br>(fm) | $a$<br>(fm) | $W$<br>(MeV) | $r_0'$<br>(fm) | $a'$<br>(fm) | Reference        |
|---------|--------------|---------------|-------------|--------------|----------------|--------------|------------------|
| Tritons |              |               |             |              |                |              |                  |
| T1      | 153          | 1.24          | 0.684       | 25.8         | 1.45           | 0.806        | 9                |
| T2      | 168          | 1.16          | 0.730       | 24.1         | 1.45           | 0.790        | 9                |
| Alphas  |              |               |             |              |                |              |                  |
| A1      | 52.9         | 1.571         | 0.533       | 11.0         | 1.571          | 0.533        | 12               |
| A2      | 153.6        | 1.468         | 0.523       | 19.8         | 1.468          | 0.523        | 12               |
| A3      | 187.3        | 1.444         | 0.523       | 22.3         | 1.444          | 0.523        | 12               |
| A4      | 187.3        | 1.25          | 0.70        | 22.3         | 1.25           | 0.70         | ... <sup>a</sup> |

<sup>a</sup> Our modifications of the optical-model set, A3, of Ref. 12 were chosen to better fit the angular distributions.

and the Coulomb potential  $V_c$  of a uniformly charged sphere of radius  $r_0^c$  is  $r_0^c A^{1/3}$ . The term  $V$  represents the real well depth,  $W$  the volume absorption term,  $r_0$  and  $r_0'$  the radius parameters, and  $a$  and  $a'$  the diffuseness parameters.

We obtained optimum values of the optical-model parameters using Perey's automatic search routine,<sup>11</sup> which searches on those parameters that are preassigned as variables until  $\chi^2$  reaches a minimum value, where

$$\chi^2 = N^{-1} \sum_{i=1}^N [\sigma_{\text{th}}(\theta_i) - R\sigma_{\text{ex}}(\theta_i)]^2 / (\Delta\sigma_{\text{ex}})^2(\theta_i). \quad (2)$$

The measured and predicted cross sections are denoted by  $\sigma_{\text{ex}}$  and  $\sigma_{\text{th}}$ , respectively;  $\Delta\sigma_{\text{ex}}$  is the error

associated with  $\sigma_{\text{ex}}$ ;  $N$  is the number of experimental points used in the fit. The normalization factor is denoted by  $R$ .

Table I presents the sets of parameters that gave the best fit to our data for 15-MeV tritons on  $^{86}\text{Sr}$ . Reference 9 includes the details of the choice of initial parameters and of the fitting procedure.

#### B. $^{85}\text{Rb}$ Levels

We measured  $\alpha$ -particle spectra from the  $^{86}\text{Sr}(t, \alpha)^{85}\text{Rb}$  reaction at  $2.5^\circ$  intervals from  $12.5$  to  $90^\circ$ . Figure 1 shows a representative spectrum.

The  $^{85}\text{Rb}$  levels observed in this study are listed in Table II. We made angular momentum assignments (labeled  $l_p$  in column 3) on the basis of

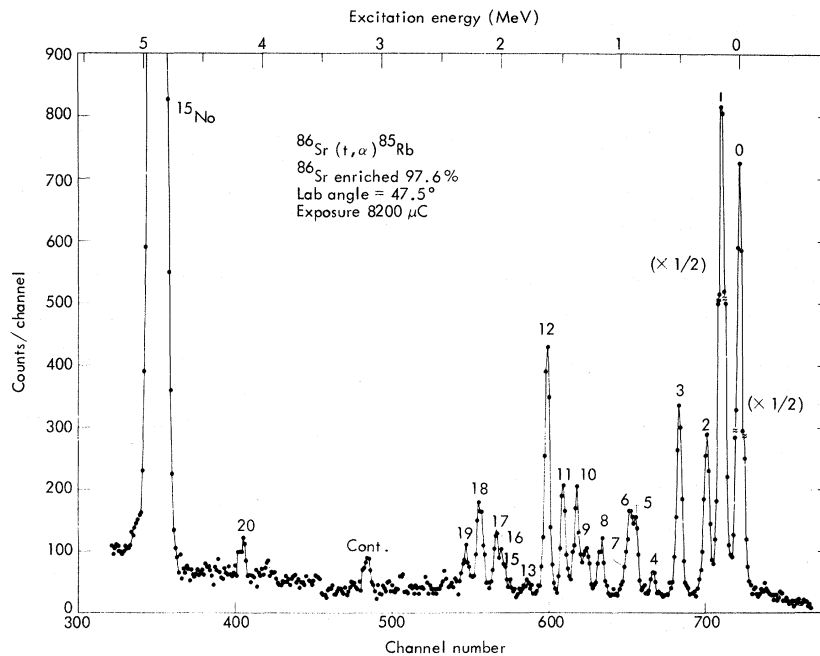


FIG. 1.  $\alpha$ -particle spectrum at laboratory angle of  $47.5^\circ$ . The numbered peaks are listed in Table II. The peak labeled "cont." is a contaminant peak.

TABLE II. Summary of states populated by  $^{86}\text{Sr}(t, \alpha)^{85}\text{Rb}$  with 15.0-MeV tritons.

| Level <sup>a</sup><br>No. | Energy <sup>b</sup><br>(keV) | $l_p$  | Parameter set T1, A4  |            |                         |            | S<br>(N=40) | Parameter set T1, A3  |            |                         |            | S<br>(N=53) |
|---------------------------|------------------------------|--------|---|------------|-------------------------|------------|-------------|---|------------|-------------------------|------------|-------------|
|                           |                              |        | $(d\sigma/d\Omega)_{\text{expt}}/(d\sigma/d\Omega)_{\text{DW}}^c$ |            |                         |            |             | $(d\sigma/d\Omega)_{\text{expt}}/(d\sigma/d\Omega)_{\text{DW}}^c$ |            |                         |            |             |
|                           |                              |        | $2p_{3/2}$  | $2p_{1/2}$ | $1f_{5/2}$              | $1g_{9/2}$ |             | $2p_{3/2}$  | $2p_{1/2}$ | $1f_{5/2}$              | $1g_{9/2}$ |             |
| 0                         | 0                            | 3      |   |            | <u>149</u>              |            | 3.73        |   |            | <u>205</u>              |            | 3.87        |
| 1                         | 151.5 ± 2                    | 1      | <u>83</u>   |            |                         |            | 2.08        | <u>96</u>   |            |                         |            | 1.81        |
| 2                         | 281 ± 2                      | 1      | 16.5  | <u>20</u>  |                         |            | 0.50        | <u>20</u>   | <u>24</u>  |                         |            | 0.45        |
| 3                         | 514 ± 3                      | 4      |   |            |                         | <u>27</u>  | 0.68        |   |            |                         | <u>39</u>  | 0.74        |
| 4                         | 732 ± 6                      | (3, 4) |   |            | <u>3.4</u>              | 1.6        | 0.09        |   |            | <u>4.7</u>              | <u>2.2</u> | 0.09        |
| 5                         | 880 ± 7                      | 1      | <u>5.8</u>  | 7.0        |                         |            | 0.15        | <u>7.5</u>  | 9.0        |                         |            | 0.14        |
| 6                         | 925 ± 10                     | 1      | <u>3.4</u>  | 4.1        |                         |            | 0.09        | <u>4.2</u>  | 5.0        |                         |            | 0.08        |
| (7)                       | 960 ± 10                     | (3, 4) |   |            | <u>7.0</u>              | 3.5        | 0.17        |   |            | <u>8.0</u>              | 4.8        | 0.15        |
| 8                         | 1172 ± 5                     | (3)    |   |            | <u>8.3</u>              |            | 0.21        |   |            | <u>13</u>               |            | 0.25        |
| 9                         | 1291 ± 7                     | 1      | <u>3.2</u>  | 3.8        |                         |            | 0.08        | <u>3.9</u>  | 4.7        |                         |            | 0.07        |
| 10                        | 1375 ± 8                     | (3, 4) |   |            | <u>12</u>               | 7.4        | 0.30        | <u>16</u>   | 10         | 16                      | 10.5       | 0.30        |
| 11                        | 1492 ± 8                     | 1      | <u>6.3</u>  | 7.6        |                         |            | 0.16        | <u>8.0</u>  | 9.6        |                         |            | 0.15        |
| 12                        | 1627 ± 4                     | 3      |   |            | <u>35</u>               |            | 0.87        |   |            | <u>49</u>               |            | 0.92        |
| 13 <sup>d</sup>           | 1792 ± 15                    | (3, 4) |   |            | <u>3.3</u>              | 2.0        | 0.08        |   |            | <u>4.8</u>              | 3.0        | 0.09        |
| (14)                      | 1891 ± 15                    |        |   |            |                         |            | (~0.10)     |   |            |                         |            | 0.12        |
| 15 <sup>d</sup>           | 1940 ± 10                    |        |   |            |                         |            | (~0.07)     |   |            |                         |            | 0.09        |
| 16                        | 2006 ± 10                    |        |   |            |                         |            | (~0.10)     |   |            |                         |            | 0.12        |
| 17                        | 2056 ± 5                     |        |   |            |                         |            | (~0.20)     |   |            |                         |            | 0.24        |
| 18                        | 2191 ± 10                    | (1)    | <u>4.6</u>  | 5.5        |                         |            | 0.12        | <u>5.7</u>  | 6.8        |                         |            | 0.10        |
| 19                        | 2304 ± 12                    |        |   |            |                         |            | (~0.13)     |   |            |                         |            | 0.16        |
| 20                        | 4195 ± 10                    | (3)    |   |            | 7.0 ( $\frac{5}{2}^-$ ) |            | 0.10        |   |            | 9.7 ( $\frac{5}{2}^-$ ) |            | 0.10        |
|                           |                              |        |   |            | 4.0 ( $\frac{7}{2}^-$ ) |            |             |   |            | 5.6 ( $\frac{7}{2}^-$ ) |            |             |

<sup>a</sup> Parentheses in this column indicate tentative  $^{85}\text{Rb}$  assignments.

<sup>b</sup> These uncertainties represent the precision of the measurements.

<sup>c</sup> Ratios underlined are those used for calculations of spectroscopic factors shown.

<sup>d</sup> Probable doublets.

agreements of the experimental angular distributions with the predicted distributions using distorted-wave Born-approximation (DWBA) analyses. The assignment of an  $l_p$  value for a level does not uniquely determine the spin assignment  $J$ , since the relative spin of the transferred proton is not known, i.e.,  $J = l_p \pm \frac{1}{2}$  whereas  $\pi = (-1)^l$

### C. Distorted-Wave Analysis

We used the computer code JULIE<sup>12</sup> to make the distorted-wave analyses. The calculations used the zero-range approximation, and the radial integrations were initiated at the nuclear center. We assumed the proton to be bound in a Woods-Saxon potential well with a binding energy equal to the experimental separation energy (9.639 MeV) and with the parameters  $r_o = 1.25$  fm and  $r_o$  (Coulomb) = 1.25 fm, spin-orbit strength  $\lambda = 25$ , and  $a$  (diffuseness) = 0.65 fm.

We made exploratory calculations to determine the best combination of triton and  $\alpha$ -particle parameters. These calculations involved several combinations of previously published  $\alpha$ -particle parameters together with our triton parameters (T1 and T2 in Table I). We used four sets of  $\alpha$ -par-

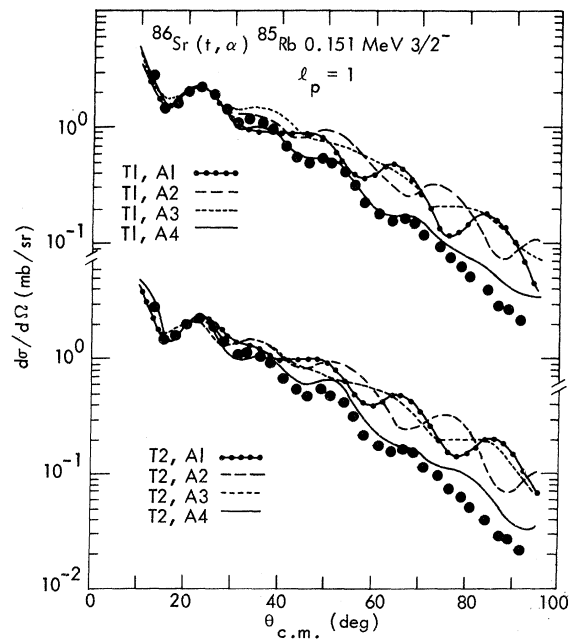


FIG. 2. Calculated angular distributions for the  $(t, \alpha)$  transition to the  $\frac{3}{2}^-$  first-excited state of  $^{85}\text{Rb}$  at 0.151 MeV. The curves correspond to combinations of triton and  $\alpha$ -particle parameters contained in Table I.

ticle parameters (shown in Table I). The sets A1, A2, and A3 are taken from optical-model fits to the elastic scattering of 24.7-MeV  $\alpha$  particles from zirconium using a four-parameter Woods-Saxon potential.<sup>13</sup> The set A4 is our modification of the set A3 to provide a better fit to the angular distributions.

The various combinations of triton and  $\alpha$ -particle parameters were tested by comparing the calculated distributions with the experimental distribution for the  $\frac{1}{2}$  level at 0.151 MeV with  $l_p = 1$  (see Fig. 2). Note that the set A4 provides a much better fit than A1, A2, or A3. While the difference in calculated cross sections between the triton sets T1 and T2 is only 3%, we have chosen to use the set T1 because it fits the data somewhat better than T2. Therefore, for all the calculated angular distributions shown in Figs. 3–5, the optical-model parameter sets T1 and A4 have been used.

For  $^{86}\text{Sr}$  the  $2p_{3/2}$ ,  $1f_{5/2}$ ,  $2p_{1/2}$ , and  $1g_{9/2}$  orbitals are the principal ones available for proton pickup to low excitations. Therefore probable  $l$  values are limited to  $l=1, 3, \text{ or } 4$ , and all comparisons have

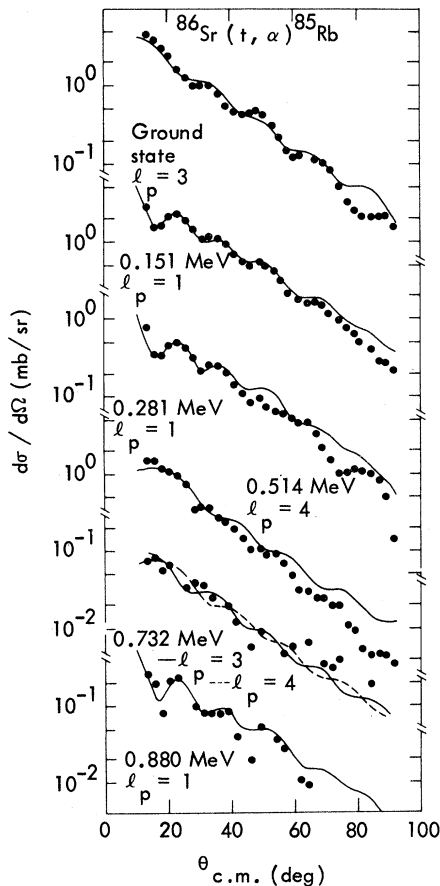


FIG. 3. Experimental angular distributions, levels 0–5, compared to the calculated DWBA curves. The relative errors are the sizes of the dots.

been made in terms of these three. The  $l=1$  distributions are easily distinguished by their distinctive minima at  $20^\circ$ . However, the  $l=3$  and  $l=4$  distributions are difficult to differentiate for weakly populated levels, as in the case of the 732-keV level. Because of the poor statistics and scatter, assignments could not be made for the levels above level 13.

The experimental and calculated DWBA cross sections for the reaction to a given  $^{85}\text{Rb}$  level were taken to be related by the expression

$$\left(\frac{d\sigma}{d\Omega}\right)_{\text{expt}} = \frac{NS(l, j)}{2j+1} \left(\frac{d\sigma}{d\Omega}\right)_{\text{DW}}, \quad (3)$$

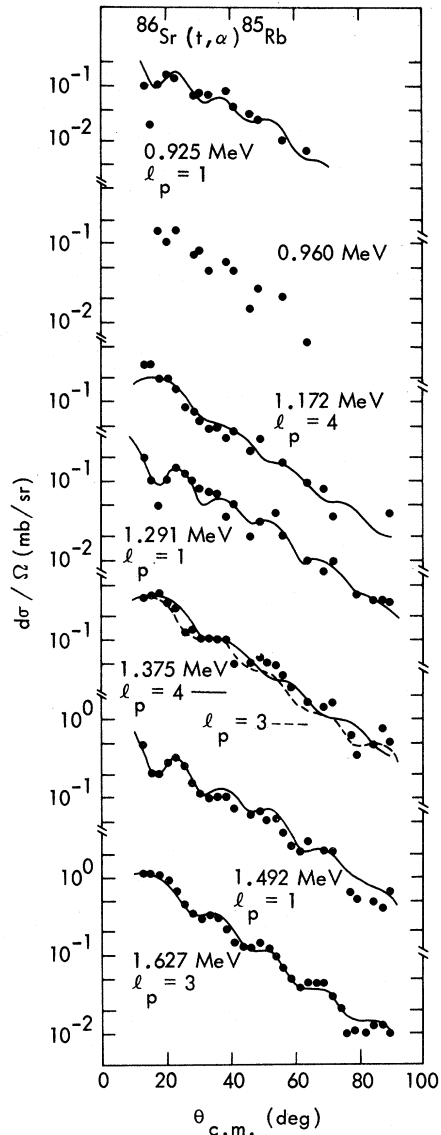


FIG. 4. Experimental angular distributions, levels 6–12, compared to the calculated DWBA curves. The relative errors are the sizes of the dots.

where  $S(l, j)$  is the spectroscopic factor and  $N$  is the normalization factor that contains the overlap of  $\alpha$  and triton. The quantities  $(d\sigma/d\Omega)_{\text{expt}} / (d\sigma/d\Omega)_{\text{DW}}$ , obtained by fitting the experimental to the calculated angular distributions over the angle range  $12.5$  to  $30^\circ$ , are listed in Table II for the parameter sets T1, A4 and T1, A3. Although the latter fits were significantly poorer, we listed them to provide an indication of the sensitivity of the spectroscopic factors to the  $\alpha$  optical parameters assumed. The values of the normalization factors  $N$  shown are approximate and were derived from sum-rule considerations with the following assumptions:

- (a) Levels 1–9, spanning the excitation region up through 2304 keV, were taken to contain all the trans- $1f_{7/2}$  strength (10 particle units) distributed amongst the orbitals  $2p_{3/2}$ ,  $2p_{1/2}$ ,  $1f_{5/2}$ , and  $1g_{9/2}$ .
- (b) All  $l_p=1$  populations except the 281-keV level were taken to be  $2p_{3/2}$  and all uncertain  $l_p=3$  or 4 populations were taken to be  $1f_{5/2}$ .
- (c) Levels 14–17 and 19, for which no  $l_p$  assignments could be made at all, were allocated an estimated strength on the basis of a crude “average” fit. With the normalization factors rounded off to  $N=40$  and  $N=53$  for the two parameter sets, the total spectroscopic strengths add up to 9.9 in each case. The arbitrariness of the second assumption had only a small effect on the normalization factor. The choice of  $2p_{1/2}$  for all the unassigned  $l_p=1$  populations would have increased the total strength (for the T1, A4 case) by only 0.1, and the choice of  $1g_{9/2}$  for all unassigned  $l_p=3, 4$  populations would have decreased the total strength by 0.3.

For the parameter set T1, A4 with a normalization factor of  $N=40$ , the sum-rule strengths are 5.5 for  $1f_{5/2}$ , 2.7 for  $2p_{3/2}$ , 0.5 for  $2p_{1/2}$ , and 0.7 for  $1g_{9/2}$ , compared to the respective simple shell-model values of 6, 4, 0, and 0. Although we are not aware of any wave-function calculations for  $^{86}\text{Sr}$ , such calculations have been made for  $^{88}\text{Sr}$ , and we can compare our  $^{86}\text{Sr}$  data with them. Hughes<sup>14</sup> has calculated the proton wave function of  $^{88}\text{Sr}$  to be

$$0.69(2p_{1/2})^{-2} + 0.21(2p_{3/2})^{-2} + 0.08(1f_{5/2})^{-2} + 0.01(1f_{7/2})^{-2}$$

based on effective interaction potentials calculated from the  $^{90}\text{Zr}$  level structure. This calculated wave function predicts sum-rule strengths of 5.5 for  $1f_{5/2}$ , 3.2 for  $2p_{3/2}$ , and 0.6 for  $2p_{1/2}$ . The  $1g_{9/2}$  orbital was not included in the calculations; however, the agreement with our results on  $^{86}\text{Sr}$  is reasonable.

The factor  $N=40$  can be compared to  $N=29$  used by Tucker *et al.*<sup>15</sup> for  $(t, \alpha)$  on  $^{87}\text{Rb}$ , to  $N=38$  used by Blair and Armstrong<sup>16</sup> for  $(t, \alpha)$  on Ni isotopes, to  $N=45$  used by Santo *et al.*<sup>17</sup> for  $(t, \alpha)$  on Ca iso-

topes, and to  $N=34$  used by Barnes *et al.*<sup>18</sup> for  $(t, \alpha)$  on  $^{210}\text{Po}$ . Note that although the normalization factor deduced for the parameter set T1, A3 is almost 40% larger than for the set T1, A4, the relative magnitudes of the spectroscopic factors for the individual levels are not so sharply affected. In any case, the choice of  $\alpha$ -particle optical-model parameters for DWBA analysis of the  $(t, \alpha)$  reactions of interest here is not expected to be well specified by  $\alpha$ -elastic scattering measurements, because of angular momentum mismatch. This mismatch, in which the semiclassical momentum transfer  $(k^\alpha - k^t)R$  exceeds the angular momentum  $l$  transferred to the nucleus, has the effect of

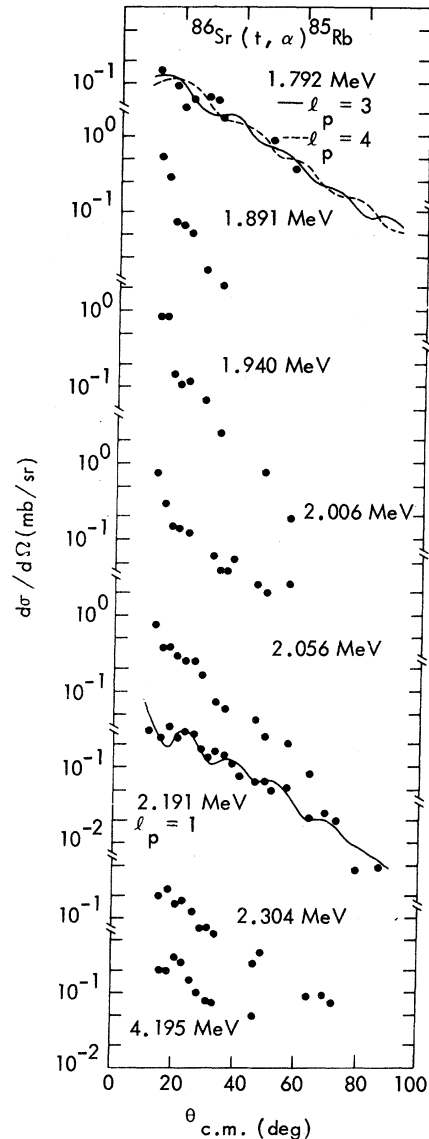


FIG. 5. Experimental angular distributions, levels 13–20, compared to the calculated DWBA curves. The relative errors are the sizes of the dots.

spreading out the range of partial waves in the  $\alpha$  and the  $t$  channels that contribute significantly to the reaction amplitude, whereas elastic scattering mainly samples the waves near the nuclear surface. In the present case the mismatch occurs below  $l \sim 4$ , and thus it involves most of the proton pickup reactions to the lower-excited levels of  $^{85}\text{Rb}$ . Although the measured sets of elastic scattering parameters do not sufficiently determine the  $(t, \alpha)$  cross sections, Stock *et al.*<sup>19</sup> have shown for the DWBA formulation employed here that the optical potentials should conform to the relationship

$$V(t, ^{86}\text{Sr}) + V(p, ^{85}\text{Rb}) \approx V(\alpha, ^{85}\text{Rb}). \quad (4)$$

Stock's analysis for  $(^3\text{He}, \alpha)$  reactions has been restated for our  $(t, \alpha)$  reaction. The potentials employed in our analysis (153, 58, and 187.3 MeV) miss Stock's criterion by 24 MeV.

#### IV. DISCUSSION

##### A. Comparison with Other Experiments

Table III compares our results on  $^{85}\text{Rb}$  levels with other data. Recently Bubb, Naqvi, and Wolfson<sup>2</sup> reported that the decay of the  $\frac{3}{2}^+$  isomer of  $^{85}\text{Sr}$  populated only the  $\frac{3}{2}^+$  level at 514.0 keV in  $^{85}\text{Rb}$ . They did not observe the  $\gamma$  rays at 880 and 356 keV that had been previously reported and assumed to deexcite a level at 880 keV (see Ref. 1). Since they could not, therefore, support the exist-

tence of a level near 880 keV populated in  $^{85}\text{Sr}$  decay, they concluded that the 870-keV level observed in Coulomb excitation experiments<sup>4</sup> was not populated in  $^{85}\text{Sr}$  decay. They further reported that the decay of the  $\frac{1}{2}^-$  isomer of  $^{85}\text{Sr}$  populated only the  $\frac{3}{2}^-$  151-keV level in  $^{85}\text{Rb}$ .

As shown in Table III, our  $l_p$  values and energies for the levels at 0, 151, 281, 514, and 880 keV are consistent with the more recent decay scheme studies<sup>3</sup> and the  $(n, n'\gamma)$  studies,<sup>6</sup> which have shown the earlier results<sup>2</sup> to be in error. However the probable  $l_p$  values for the 732-keV level disagree with the decay data; our angular distributions definitely do not fit  $l_p = 1$ , as would appear to be required. We suspect that the "732-keV level" we observe is an unresolved doublet. For the higher-lying levels the energy agreements with the  $(n, n'\gamma)$  results<sup>6</sup> are satisfactory.

##### B. Level Structure of $^{85}\text{Rb}$

Figure 6 compares the low-energy level structures<sup>20-24</sup> of the odd- $A$  rubidium isotopes. The numbers on the right side of the levels indicate the  $l$  value for the proton pickup reaction. Note that the ground-state spins of all the odd- $A$  gallium, arsenic, bromine, and rubidium isotopes are  $\frac{3}{2}^-$  with the exception of  $^{83}\text{Rb}$  and  $^{85}\text{Rb}$ , which are  $\frac{5}{2}^-$ . This anomaly has been reproduced only with calculations based on the Coriolis-coupling model and a

TABLE III. Population of  $^{85}\text{Rb}$  levels.

| $^{86}\text{Sr}(t, \alpha)$<br>Energy | $l_p$  | S   | Energy<br>(keV) | $J^\pi$           | Decay data <sup>a</sup>                    |  |  |  | $^{85}\text{Rb}(n, n'\gamma)$ <sup>b</sup> |                   |
|---------------------------------------|--------|-----|-----------------|-------------------|--|--|--|--|--|-------------------|
|                                       |        |     |                 |                   | $^{85}\text{Kr}^m$<br>$\text{Log}_{10} ft$ | $^{85}\text{Kr}^s$<br>$\text{Log}_{10} ft$ | $^{85}\text{Sr}^m$<br>$\text{Log}_{10} ft$ | $^{85}\text{Sr}^s$<br>$\text{Log}_{10} ft$ | Energy                                     | $J^\pi$           |
| 0                                     | 3      | 3.7 | 0               | $\frac{5}{2}^-$   |  | 9.1  |  |  | 0  | $\frac{5}{2}^-$   |
| 151.5                                 | 1      | 2.1 | 151.18          | $\frac{3}{2}^-$   | 5.2  |  | 4.4  |  | 151  | $\frac{3}{2}^-$   |
| 281                                   | 1      | 0.5 | 281.04          | $\frac{1}{2}^-$   | 7.4  | 16.3                                       | 6.4  |  | 280  | $(\frac{1}{2}^-)$ |
| 514                                   | 4      | 0.7 | 513.99          | $\frac{3}{2}^+$   |  | 9.3  |  | 6.1  | 514  | $(\frac{3}{2}^+)$ |
| 732                                   | (3, 4) | 0.1 | 731.9           | $(\frac{3}{2})^-$ | 6.8  |  | 6.4  |  | 731  |                   |
|                                       |        |     | 868.05          | $\frac{7}{2}^-$   |  |  |  | 8.8  | 869  |                   |
| 880                                   | 1      | 0.2 | 880.            |                   |  |  | > 8.9                                      | > 12                                       |  |                   |
| 925                                   | 1      | 0.1 |                 |                   |  |  |  |  | 919  |                   |
| 960                                   | (3, 4) | 0.2 |                 |                   |  |  |  |  | 951  |                   |
| 1172                                  | (3)    | 0.2 |                 |                   |  |  |  |  | 1175                                       |                   |
| 1291                                  | 1      | 0.1 |                 |                   |  |  |  |  | 1294                                       |                   |
| 1375                                  | (3, 4) |     |                 |                   |  |  |  |  | 1383                                       |                   |
|                                       |        |     |                 |                   |  |  |  |  | 1445                                       |                   |
| 1492                                  | 1      | 0.2 |                 |                   |  |  |  |  |  |                   |

<sup>a</sup> Decay data from Ref. 3.

<sup>b</sup> Reference 6.

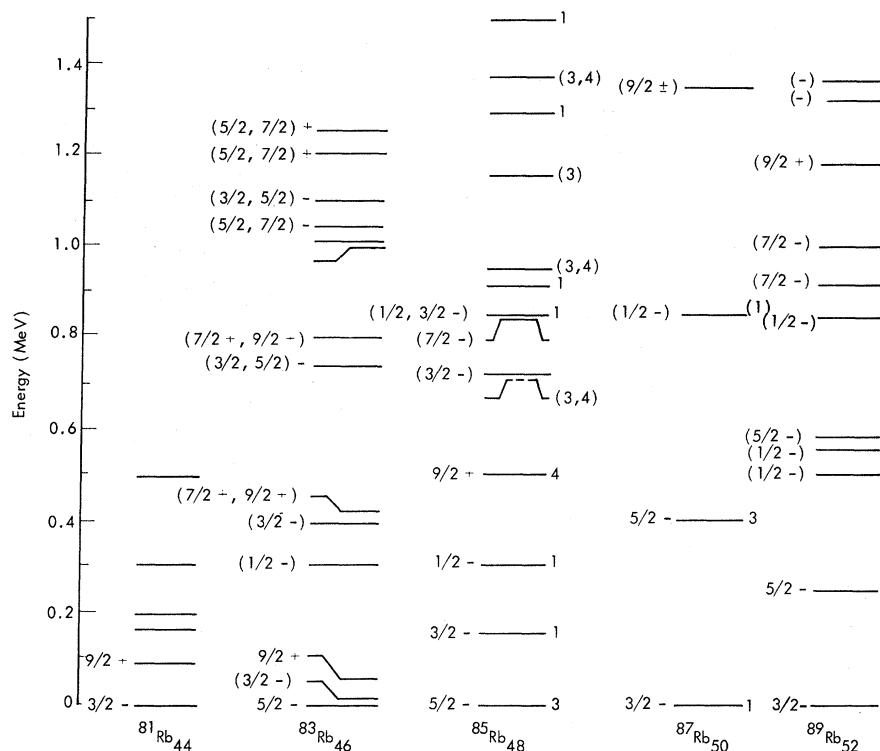


FIG. 6. Low-energy structures of the odd- $A$  rubidium isotopes. Data taken from Ref. 1, Ref. 20 ( $^{83}\text{Rb}$ ), Refs. 21, 22 ( $^{87}\text{Rb}$ ), and Refs. 23, 24 ( $^{89}\text{Rb}$ ). Numbers to the right of levels indicate  $l$  value for the proton pickup reaction.

pairing-type residual interaction<sup>7</sup> within a deformed framework. These structures do not follow the predictions of the simple shell model: a  $p_{3/2}$  proton-hole ground state for the odd- $A$  rubidium isotopes. Rather, the  $^{85}\text{Rb}$  ground state is apparently composed mostly by the  $1f_{5/2}$  proton-hole configuration.

A qualitative comparison of the  $^{85}\text{Rb}$  level structure with the weak-coupling model of de-Shalit<sup>25</sup> can be made by considering the coupling of single-particle states with  $^{84}\text{Kr}$  or  $^{86}\text{Sr}$  collective excitations. The  $2_1^+$  states in  $^{84}\text{Kr}$  and  $^{86}\text{Sr}$  lie at 883 and 1078 keV, respectively. Coupling of a  $2^+$  core state with a  $1f_{5/2}^{-1}$  single hole should produce a quintet of levels of odd parity at a mean excitation energy of  $\sim 0.9$  MeV with spins  $\frac{1}{2}^- \rightarrow \frac{9}{2}^-$ . The levels at 732, 880, 925, and 960 keV, then, would contain strong components of such a coupling. Close

agreement with the model is not expected since it has already been demonstrated that the  $2^+$  states of  $^{84}\text{Kr}$  and  $^{86}\text{Sr}$  are best described by excitations intermediate between those of pure two-quasi-particle character and of pure collective character.<sup>26</sup>

#### ACKNOWLEDGMENTS

We thank W. A. Sedlacek for developing a technique for preparing  $^{86}\text{Sr}$  targets by molecular plating of strontium on thin carbon foils and I. K. Kressin and L. D. Allen for preparing the evaporated  $^{86}\text{Sr}$  targets. We appreciate the considerable work done by the Los Alamos Scientific Laboratory Van de Graaff staff in providing the beams and many of the facilities for our experiments. We also express our appreciation to G. A. Cowan for his interest and support and to W. E. Nervik for his continuing encouragement.

\*Work performed under the auspices of the U. S. Atomic Energy Commission.

<sup>1</sup>D. J. Horen, Nucl. Data B5, 131 (1971).

<sup>2</sup>I. F. Bubb, S. I. H. Naqvi, and J. L. Wolfson, Bull. Am. Phys. Soc. 15, 757 (1970).

<sup>3</sup>R. C. Ragaini, C. F. Smith, and R. A. Meyer, Bull. Am. Phys. Soc. 17, 444 (1972).

<sup>4</sup>D. S. Andreev, L. N. Gal'perin, A. Z. Il'yasov, I. Kh.

Lemberg, and I. N. Chuginov, Izv. Akad. Nauk SSSR, Ser. Fiz. 32, 226 (1968) [transl.: Bull. Acad. Sci. USSR Phys. Ser. 32, 205 (1968)].

<sup>5</sup>P. Bond and G. Kumbartski, Stanford University, private communication.

<sup>6</sup>R. P. Torti, V. M. Cottles, V. R. Dave, J. A. Nelson, and R. M. Wilenzick, Phys. Rev. C 6, 1686 (1972).

<sup>7</sup>W. Scholz and F. B. Malik, Phys. Rev. 176, 1355 (1968).

- <sup>8</sup>D. D. Armstrong, J. G. Beery, E. R. Flynn, W. S. Hall, P. W. Keaton, Jr., and M. P. Kellogg, *Nucl. Instrum. Methods* **70**, 69 (1969).
- <sup>9</sup>R. C. Ragaini, J. D. Knight, and W. T. Leland, *Phys. Rev. C* **2**, 1020 (1970).
- <sup>10</sup>A. H. Wapstra and N. B. Gove, *Nucl. Data* **B9**, 267 (1971).
- <sup>11</sup>F. G. Perey, *Phys. Rev.* **131**, 745 (1963).
- <sup>12</sup>R. H. Bassel, R. M. Drisko, and G. R. Satchler, Oak Ridge National Laboratory Report No. ORNL-3240 (1962).
- <sup>13</sup>L. McFadden and G. R. Satchler, *Nucl. Phys.* **84**, 177 (1966).
- <sup>14</sup>T. A. Hughes, *Phys. Rev.* **181**, 1586 (1969).
- <sup>15</sup>A. B. Tucker, K. E. Apt, J. D. Knight, and C. J. Orth, *Phys. Rev. C* **6**, 2075 (1972).
- <sup>16</sup>A. G. Blair and D. D. Armstrong, *Phys. Rev.* **151**, 930 (1966).
- <sup>17</sup>R. Santo *et al.*, *Nucl. Phys.* **A118**, 409 (1968).
- <sup>18</sup>P. D. Barnes *et al.*, *Nucl. Phys.* **A195**, 146 (1972).
- <sup>19</sup>R. Stock, R. Bock, P. David, H. H. Duhm, and T. Tamura, *Nucl. Phys.* **A104**, 136 (1967).
- <sup>20</sup>R. C. Etherton, L. M. Beyer, W. H. Kelley, and D. J. Horen, *Phys. Rev.* **168**, 1249 (1968).
- <sup>21</sup>A. Shihab-Eldin, S. G. Prussin, F. M. Bernthal, and J. O. Rasmussen, *Nucl. Phys.* **A160**, 33 (1971).
- <sup>22</sup>C. D. Kavaloski, J. S. Tilley, D. C. Shreve, and N. Stein, *Phys. Rev.* **161**, 1107 (1967).
- <sup>23</sup>W. F. F. Poehlman, B. Singh, and M. W. Johns, *Can. J. Phys.* **50**, 2741 (1972).
- <sup>24</sup>E. A. Henry and W. L. Talbert, Jr., *Phys. Rev. C* **7**, 222 (1973).
- <sup>25</sup>A. DeShalit, *Phys. Rev.* **122**, 1530 (1961).
- <sup>26</sup>S. Wahlborn, *Nucl. Phys.* **58**, 209 (1964).